

# Design and Optimisation of a Modular PV-CSP Hybrid Plant

Benjamin Gardiner<sup>1</sup> , Stephen Clark<sup>1</sup> , and Craig McGregor<sup>1,\*</sup> 

<sup>1</sup>Stellenbosch University, South Africa

\*Correspondence: Craig McGregor, craigm@sun.ac.za

**Abstract.** This study investigates the design and optimisation of a hybrid plant comprising an array of 30 MW<sub>ac</sub> PV-CSP modules. Each module integrates a PV system, a power tower CSP with thermal energy storage, and a gas-fired generator for backup power. This configuration aims to leverage the benefits of both PV and CSP technologies while addressing the challenges associated with large-scale CSP systems, such as high upfront costs and lengthy construction periods. A Python-based application was developed to optimise and simulate a modular PV-CSP hybrid plant. This application integrates existing software with custom computational and financial models to generate performance and economic metrics. These metrics were used to compare a single 120 MW<sub>ac</sub> plant with a modular plant comprising 4 x 30 MW<sub>ac</sub> modules that are constructed sequentially. The large-scale plant demonstrates better economic performance across all investigated metrics. The modular layout enables earlier revenue generation; however, it has a higher total installation cost than the large-scale plant. These findings highlight the possible economic advantages of constructing single large-scale systems rather than integrating several small-scale systems.

**Keywords:** Modular, PV-CSP, Hybrid

## 1. Introduction

### 1.1 Background

Climate change has resulted in several global decarbonisation initiatives, including the Paris Agreement [1], which necessitate a transition to renewable energy sources such as solar and wind energy. Solar photovoltaic (PV) technology accounts for approximately 60% of the global renewable energy capacity additions between 2014 and 2023 [2]. This can be primarily attributed to its rapidly decreasing levelised cost of electricity (LCOE) [3]. While PV technology is cost-effective, its output is limited to sunlight hours and is variable without energy storage. Installing additional PV capacity without mitigating this variability can result in several drawbacks such as curtailment, diminishing returns, and the “duck-curve” phenomenon [4]. To address this challenge, one approach is to store generated PV electricity in a battery energy storage system (BESS); however, these are expensive in large-scale utility projects [5]. Alternatively, a PV system can be combined with a flexible power generation system, such as concentrating solar power (CSP) technology. This hybrid approach leverages the lower energy production cost of PV technology with the operational flexibility and lower storage costs of CSP technology. A study conducted by Schöniger et al. [6] indicates that CSP with thermal energy storage (TES) is currently cheaper than PV with a BESS when more than 4 hours of storage is used. However, some of the biggest challenges of establishing a CSP system is the long construction time and large upfront capital required to construct it.

A CSP plant data set compiled by Thonig et al. [7] indicates that conventional CSP plants are constructed in 2 to 4 years and require investments of billions of U.S dollars. These challenges can be mitigated by utilising a modular plant layout. A modular layout integrates several smaller-scale systems to collectively achieve the same capacity as a single, large-scale system. This modular approach offers several advantages. Firstly, within constraints, each individual module has a shorter construction period. This enables earlier revenue generation and improved cash flows, thereby increasing return on investment. Secondly, a modular layout is less susceptible to single points of failure. If one module experiences an issue, the remaining modules can continue generating electricity. This mitigates the risk of complete plant shutdown and associated revenue losses, as highlighted by an incident reported at the Noor III CSP plant [8].

The advantages discussed above highlight an opportunity to investigate a hybrid plant comprising an array of PV-CSP modules. However, there may still be prolonged periods with no sunlight, during which neither the PV nor the CSP systems can generate electricity. A study conducted by Clark and McGregor [9] defines and confirms the necessity of firm-dispatchable generation to fully support the energy demand met by variable supply sources. Therefore, it is beneficial for each module to incorporate a gas-fired generator to provide backup power during periods of low or no solar radiation. This can ensure continuous baseload power generation to enhance the overall reliability of the plant.

## 1.2 Research objectives

This study seeks to leverage the benefits of both PV and CSP technologies while addressing the challenges associated with large-scale CSP systems, such as high upfront costs and lengthy construction periods. Hence, this study investigates the design and optimisation of a hybrid plant comprising an array of PV-CSP modules, augmented with a gas-fired generator for backup power. Moreover, each CSP system has its own dedicated TES system and power block. This hybrid plant configuration aims to ensure reliable, dispatchable baseload electricity generation while reducing implementation barriers and improving economic feasibility.

## 1.3 Project scope

The economic feasibility and performance of a solar power plant are intrinsically linked to its geographic location due to variations in solar resource, energy tariffs, and market conditions. To provide a more focused analysis, this study limits exploring the design and optimisation of a hybrid plant located in South Africa. Moreover, this study investigates the primary systems and subsystems of the hybrid plant with a level of detail sufficient for the intended analysis. A comprehensive, in-depth examination of each subsystem is beyond the scope of this project.

# 2. Design basis

## 2.1 Plant design assumptions

The following assumptions are made for the plant design:

- The site of the plant is Postmasburg, South Africa. The Redstone CSP plant is currently under construction at this site and is co-located with a PV plant. This demonstrates the location's suitability for the hybrid plant. The typical meteorological year (TMY) data for the selected site was sourced from the ClimateOneBuilding repository [10].
- The plant's design conditions were based on the conditions at noon on the summer solstice. Solar noon has a local time of 12h24 on the summer solstice; however, the TMY data has an hourly resolution. Therefore, noon was selected for the design-point.
- The off-taker is assumed to have a 24-hour constant baseload requirement.
- This study restricts its scope to proven, well-established power tower CSP technology.

## 2.2 Module nominal capacity

Supply-cost data compiled by EPRI [11] indicates that larger capacity PV and gas-fired systems benefit from economies of scale. Therefore, larger PV systems and gas-fired units are preferred. Despite CSP technologies also benefitting from economies of scale [12], this study aims to investigate a modular layout to address the challenges associated with large-scale CSP systems. Therefore, the module's capacity was selected based on construction time rather than leveraging economies of scale.

PV systems with capacities under 99.5 MW<sub>ac</sub> require 12 months to construct in South Africa [11]. The Hami CSP plant's project timeline [13] [14] and SolarPILOT [15] were used to determine that the largest CSP system capacity that requires 12 months to construct in South Africa is 30 MW<sub>ac</sub>. Therefore, each module was selected to have a nominal capacity of 30 MW<sub>ac</sub>. This ensures that the construction of both the PV and CSP systems are completed simultaneously.

While the module capacity remains fixed, the PV system capacity, CSP system capacity, full load storage hours (FLSH), and solar multiple were iteratively adjusted within defined ranges to identify the configuration that minimises the module's LCOE. In contrast, the capacity of the gas-fired generator is fixed at 30 MW<sub>ac</sub>, matching the selected module capacity. This ensures that the gas-fired generator can provide full backup power when solar resources are insufficient and neither the PV nor CSP systems are generating electricity.

## 2.3 Dispatch strategy

Each module dispatches electricity according to the following guidelines:

- The PV system dispatches power as produced.
- The CSP system stores thermal energy between 10h00 to 15h00, whilst maintaining a minimum turbine fraction of 25% to mitigate the number of annual startup procedures.
- The CSP system supplements PV output to satisfy the full load requirement between 7h00 to 9h00, and 16h00 to 19h00.
- After evening peak load, the CSP system reserves TES capacity to service the morning peak load and then evenly distributes remaining capacity between 20h00 and 6h00.
- The gas-fired generator dispatches electricity when the combined output of both PV and CSP systems cannot satisfy the full load requirement.

## 3. Modelling

### 3.1 Module modelling approach

A Python-based application was developed to optimise and simulate a modular PV-CSP hybrid plant. This application integrates existing software with custom computational and financial models to generate performance and economic metrics. These metrics were used to evaluate the economic feasibility of the plant and compare a modular system with a single large-scale system. Figure 1 illustrates the PV-CSP module simulation workflow.

The application integrates two interfaces: PySAM [16], an application programmable interface (API) for the System Advisor Model (SAM), to generate and simulate the PV system; and CoPilot [15], an API for SolarPILOT, to generate and simulate the CSP collector field. The collector field receiver dimensions and tower height were iteratively adjusted within defined ranges to identify the configuration that minimises the specific cost of thermal energy generation.

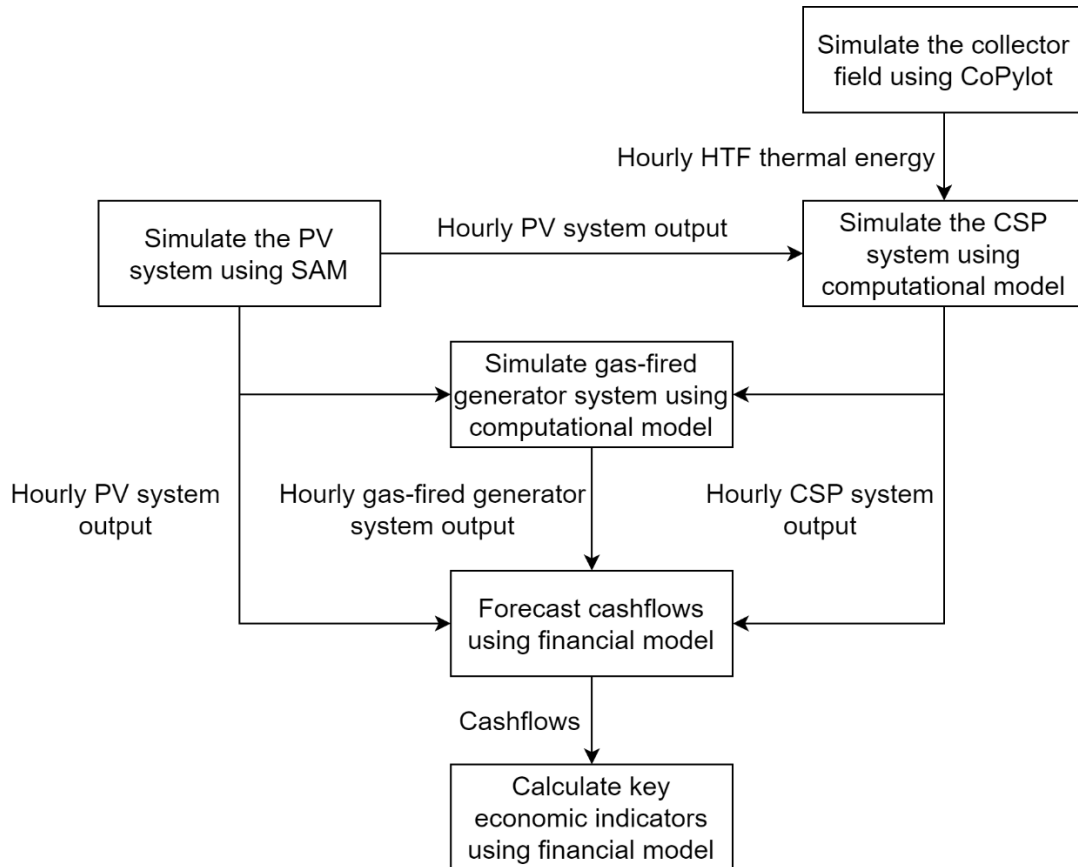


**Figure 1.** Simulation workflow for a single 30 MW<sub>ac</sub> module.

A custom Python-based computational model evaluates the hourly PV system output, and heat transfer fluid (HTF) thermal energy output from the collector field and simulates the CSP system using the dispatch strategy defined in Section 2.3. The computational model evaluates the hourly output of both the PV and CSP systems and calculates the gas-fired generator output required to maintain continuous baseload power generation.

A custom Python-based financial model evaluates the annual output and costs of the power generation systems and calculates cashflows for a defined analysis period. The model uses these cashflows to compute key economic indicators: net-present value (NPV), internal rate of return (IRR), and debt service coverage ratio (DSCR).

## 3.2 Computational model

### 3.2.1 Computational model approach

A custom Python-based computational model was developed to simulate the operation of a CSP system with TES, and to calculate the gas-generator system output required to maintain continuous baseload power generation. The model approach follows the control strategy defined by Stine and Geyer [17]. Additional startup procedure functionality incorporated in the SAM software was implemented using custom Python functions.

The model first calculates the hourly thermal energy requirement of the power block by evaluating the hourly PV system output and dispatch strategy discussed in Section 2.3. It then evaluates the collector field HTF thermal energy output and compares it to the power block's requirements. If there is excess energy, it attempts to store it in the TES system or discards it if the hot tank is full. If there is no excess energy, the power block consumes the collector field output. If the collector field cannot satisfy the power block's requirement, the TES attempts to discharge thermal energy to supplement the deficit.

The model initiates a shutdown procedure if neither the collector field nor TES provide thermal energy. To resume operation from shutdown, the receiver and power block must consume a minimum thermal energy threshold. The heliostat field initiates a shutdown procedure if no direct normal irradiance (DNI) is detected. The heliostat field requires 1 hour to startup once DNI is detected again.

The model computes hourly gross output using the power block's thermal energy input and cycle efficiency. The net output is calculated by subtracting parasitic loads from the gross output. Finally, the net output and PV system output are used to calculate the gas-generator system output required to maintain continuous baseload power generation.

### 3.2.2 CSP computational model validation

The computational model was validated using the SAM software. Table 1 displays the annual net output difference between CSP systems simulated using the computational model and the SAM software.

*Table 1. Comparison between CSP systems simulated with the computational model and SAM.*

CSP system simulation	Simulation 1	Simulation 2	Simulation 3
System capacity (MW <sub>ac</sub> )	30	80	120
Solar multiple	3.4	2.8	2.4
FLSH (hr)	16	12	8
Model net output (GWh <sub>ac</sub> )	213	486	624
SAM net output (GWh <sub>ac</sub> )	218	496	634
Difference (%)	-2.3	-1.9	-1.6

### 3.3 Financial model

A custom Python-based financial model evaluates the annual output and costs of the power generation systems and calculates cashflows for a defined analysis period. The model uses the 'numpy-financial' package [18] to calculate the plant's NPV, and IRR. The DSCR is calculated using a custom Python function. Table 2 displays the key financial model input assumptions.

*Table 2. Key financial model input assumptions.*

Metric	Value
Analysis period duration (years)	25
Investor equity (% of total installation cost)	25
Gearing (% of total installation cost)	75
PPA price (\$USD / kW <sub>ac</sub> )	0.15
Loan tenor (years)	18
Annual loan interest rate (%)	4
Discount factor (%)	7

## 4. Module design details and simulation results

### 4.1 PV system

Crystalline silicon (c-Si) PV panels were selected, with single-axis tracking capabilities. According to the independent power producer (IPP) project database [19], these are the predominant technologies for PV systems in South Africa.

The PV system was generated and simulated using the SAM PVWatts model [20]. Table 3 displays the key PV system simulation input parameters. The cost data was sourced from a supply-cost report compiled by EPRI [11].

**Table 3.** Key PV system simulation parameters.

Metric	Value
System nameplate capacity (MW <sub>ac</sub> )	34
Module type	Premium (crystalline Silicon)
Inverter efficiency (%)	96
Array type	1-axis tracking
Azimuth (°)	0 (North-facing)
Ground coverage ratio	0.3
Total system loss (%)	14
Total overnight cost (\$USD / kW <sub>ac</sub> )	1183
Fixed OPEX (\$USD / kW <sub>ac</sub> )	14

## 4.2 CSP system

A power tower CSP system was selected, with molten salt as the HTF and a conventional direct 2-tank TES system. A typical superheated steam Rankine cycle was selected for the power generation cycle in the power block. Moreover, an air-cooled condenser (ACC) was selected for the condenser due to the arid conditions of the selected plant site. The Stellio model properties were used for the collector field heliostats [21]. Table 4 displays the key CSP system simulation input parameters. The cost data was sourced from Turchi et al. [22] and Kurup et al. [21].

**Table 4.** Key CSP system simulation input parameters.

Metric	Value
Design-point DNI (W/m <sub>2</sub> )	803
Ambient dry-bulb temperature (°C)	28.1
Solar multiple	2.4
Receiver thermal power (MW <sub>th</sub> )	175
HTF hot temperature (°C)	574
HTF cold temperature (°C)	290
Full load hours of storage (hr)	16
TES thermal capacity (MWh <sub>th</sub> )	1165
Design turbine gross output (MW <sub>ac</sub> )	30
Cycle thermal efficiency (%)	41.2
Cycle thermal power (MW <sub>th</sub> )	73
Single heliostat area (m <sub>2</sub> )	48.5
Ratio of reflective area to profile (%)	97
Receiver height (m)	5
Receiver diameter (m)	6
Tower height (m)	135
Site improvement cost (\$USD / m <sup>2</sup> )	16
Heliostat field cost (\$USD / m <sup>2</sup> )	127
TES cost (\$USD / kWh <sub>th</sub> )	22
Power cycle cost (\$USD / kW <sub>ac</sub> )	1360
Balance of plant cost (\$USD / kW <sub>ac</sub> )	290
Fixed OPEX (\$USD / kW <sub>ac</sub> )	66
Variable OPEX (\$USD / MWh <sub>ac</sub> )	3.5

The tower and receiver costs were calculated according to Kistler [23] and adjusted for inflation using the Chemical Engineering Plant Cost Index (CECPI) [24]. The power block cost for a 115 MW<sub>ac</sub> steam turbine was obtained from Turchi et al. [22] and escalated to account for economies of scale, resulting in a power block specific cost of \$USD 1360 / kW<sub>ac</sub>.

### 4.3 Gas-fired generator system

The gas-generators were selected to be internal combustion engines (ICEs). Both open-cycle gas turbines (OCGTs) and ICEs power generation systems are used in South Africa. However, construction data indicates that ICEs can be constructed in 12 months in South Africa, whereas OCGTs require 24-36 months [11], [25]. The shorter construction time for ICEs aligns with the 12-month construction timeline for the PV and CSP systems, ensuring all components of the module can be completed simultaneously.

Liquefied petroleum gas (LPG) was selected for the gas-generator's fuel. Diesel is currently the predominant fuel used in South African peaking plants. However, a study by Clark et al. [26] demonstrates that LPG is more cost-effective than diesel in South Africa. Furthermore, according to carbon emission data compiled by the U.S. EIA [27], burning LPG produces approximately 15% less CO<sub>2</sub> emissions compared to burning diesel.

A typical ICE gas-generator system was simulated using a custom Python-based computational model. Table 5 summarises the gas-generator system simulation input parameters. The CAPEX and OPEX data were sourced from a supply-cost report compiled by EPRI [11]. The fuel cost was determined from the South African maximum LPG refinery gate price [28]. This refinery cost was escalated by 60% to account for levies, taxes, and margins. This escalation matches the proportional increase of South African base diesel prices [29].

**Table 5.** Key gas-fired generator simulation input parameters.

Metric	Value
System nameplate capacity (MW <sub>ac</sub> )	30
Total overnight cost (\$USD / kW <sub>ac</sub> )	2330
Fixed OPEX (\$USD / kW <sub>ac</sub> )	42
Variable OPEX (\$USD / MWh <sub>ac</sub> )	6
Fuel cost (\$USD / litre)	0.67

### 4.4 Simulation results

Table 6 summarises the simulation results of a single 30 MW<sub>ac</sub> module.

**Table 6.** Summarised simulation results of a single 30 MW<sub>ac</sub> module.

Metric	PV System	CSP System	Gas-fired Generator	Total
Net generation (GWh <sub>ac</sub> )	86	143.5	33.5	263
Capacity factor (%)	33	54	13	100
CAPEX (million \$USD)	40	191	70	301
Annual OPEX (million \$USD)	0.5	2.3	1.5	4.3
Annual Fuel costs (million \$USD)	0	0	7.5	7.5

## 4.5 Modular and single plant layout comparison

To investigate the possible economic advantages of a modular plant, a single 120 MW<sub>ac</sub> plant was compared with a modular plant comprising 4 x 30 MW<sub>ac</sub> modules that are constructed sequentially. The single large-scale plant was assumed to require 4 years to construct, which aligns with construction data for CSP systems with a similar size in South Africa [11]. In contrast, each 30 MW<sub>ac</sub> module of the modular plant was assumed to require 1 year for construction. Each layout generates approximately 1050 GWh<sub>ac</sub> of electricity annually. Table 7 summarises the economic comparison between a single 120 MW<sub>ac</sub> plant and a modular plant comprising 4 x 30 MW<sub>ac</sub> modules.

**Table 7.** Comparison between a single and modular plant layout.

Result	Single Plant Layout	Modular Plant Layout
Total installation cost (million \$USD)	1112	1204
LCOE (\$USD / MWh <sub>ac</sub> )	133	143
Debt service coverage ratio (DSCR)	1.57	1.5
Net-present value with a 7% discount factor (million \$USD)	237	197
Internal rate of return (%)	13.3	12.9

## 5. Conclusion

Based on the results shown in Table 7, the large-scale plant demonstrates better economic performance across all investigated metrics. Despite the earlier revenue generation of the modular layout, it has a higher total installation cost than the large-scale plant. This higher installation cost results in a higher LCOE, lower NPV, and lower IRR compared to the large-scale plant. These findings highlight the possible economic advantages of constructing single large-scale systems rather than integrating several small-scale systems.

## Data availability statement

Data is available on request.

## Author contributions

Investigation and writing by Benjamin Gardiner, review and editing by Craig McGregor and Stephen Clark. Conceptualisation and funding by Craig McGregor.

## Competing interests

The authors declare that they have no competing interests.

## Funding

This work is partially funded by the Department of Science and Innovation of South Africa, via the Solar Thermal Energy Research Group (STERG) within the Mechanical & Mechatronic Engineering department at Stellenbosch University.

## References

- [1] United Nations, "Paris Agreement." 2015. [Online]. Available: [https://unfccc.int/sites/default/files/english\\_paris\\_agreement.pdf](https://unfccc.int/sites/default/files/english_paris_agreement.pdf)
- [2] IRENA, "Renewable energy statistics 2024." International Renewable Energy Agency, Abu Dhabi, Jul. 2024
- [3] IRENA and CPI, "Global landscape of renewable energy finance, 2023." International Renewable Energy Agency, Abu Dhabi, 2023. [Online]. Available: [https://www.irena.org/-/media/Files/IRENA/Agency/Publication/2023/Feb/IRENA\\_CPI\\_Global\\_RE\\_finance\\_2023.pdf](https://www.irena.org/-/media/Files/IRENA/Agency/Publication/2023/Feb/IRENA_CPI_Global_RE_finance_2023.pdf)
- [4] P. Denholm, K. Clark, and M. O'Connell, "Emerging Issues and Challenges in Integrating High Levels of Solar into the Electrical Generation and Transmission System," Gold. CO Natl. Renew. Energy Lab., 2016.
- [5] W. Cole, A. W. Frazier, and C. Augustine, "Cost projections for utility-scale battery storage: 2021 update." National Renewable Energy Lab.(NREL), Golden, CO (United States), 2021.
- [6] F. Schöniger, R. Thonig, G. Resch, and J. Lilliestam, "Making the sun shine at night: comparing the cost of dispatchable concentrating solar power and photovoltaics with storage," Taylor Francis, vol. 16, no. 1, pp. 55--74, 2021
- [7] R. Thonig, A. Gilmanova, and J. Lilliestam, "CSP.guru." Jul. 01, 2023. doi: <https://doi.org/10.5281/zenodo.1318151>.
- [8] A. Erraji, "Noor III Solar Power Plant Shuts Down Until November 2024," Morroco World News, Mar. 24, 2024. [Online]. Available: <https://www.moroccoworld-news.com/2024/03/361589/noor-iii-solar-power-plant-shuts-downuntil-november-2024>
- [9] S. Clark and C. McGregor, "Firm-Dispatchable Power and its Requirement in a Power System based on Variable Generation," Mar. 2024, doi: <https://doi.org/10.48550/arXiv.2403.10869>.
- [10] L. Lawrie and D. Crawley, "Development of Global Typical Meteorological Years (TMYx)." 2022. [Online]. Available: <http://climate.onebuilding.org>
- [11] "Supply-Side Cost and Performance Data for Eskom Integrated Resource Planning," EPRI, Technical Report, 2021.
- [12] A. Fontalvo, A. Shirazi, and J. Pye, "System-level simulation of molten salt small-scale CSP," AIP Conf. Proc., vol. 2303, no. 1, p. 030015, Dec. 2020, doi: [10.1063/5.0031083](https://doi.org/10.1063/5.0031083).
- [13] T. Keck et al., "Hami – The first Stellio solar field,"
- [14] T. Keck, J. Gracia, I. Eizaguirre, D. Sun, M. Balz, and J. Iriondo, "Solar field experiences from Hami solar tower project," AIP, May 2022. doi: <https://doi.org/10.1063/5.0086590>.
- [15] M. J. Wagner and T. Wendelin, "SolarPILOT - Solar Power tower Integrated Layout and Optimization Tool," Sol. Energy, vol. 171, pp. 185–196, 2018, doi: <https://doi.org/10.1016/j.solener.2018.06.063>.
- [16] National Renewable Energy Laboratory, PySAM. (2022). [Online]. Available: <https://nrel-pysam.readthedocs.io/en/main/overview.html>
- [17] W. B. Stine and M. Geyer, Power From The Sun. 2001. [Online]. Available: <http://www.powerfromthesun.net/Book/chapter14/chapter14.html>
- [18] numpy-financial. (2022). [Online]. Available: <https://numpy.org/numpy-financial/latest/>
- [19] South African Department of Mineral Resources and Energy, "IPP Project Database." 2024. [Online]. Available: <https://www.ipp-projects.co.za/ProjectDatabase>
- [20] National Renewable Energy Laboratory, PvwattsV8. (2022). [Online]. Available: <https://nrel-pysam.readthedocs.io/en/main/modules/PvwattsV8.html>
- [21] P. Kurup, S. Akar, S. Glynn, C. Augustine, and P. Davenport, "Cost Update: Commercial and Advanced Heliostat Collectors," National Renewable Energy Laboratory, Technical Report, Feb. 2022. [Online]. Available: <https://www.nrel.gov/docs/fy22osti/80482.pdf>
- [22] C. S. Turchi et al., "CSP Systems Analysis - Final Project Report," National Renewable Energy Laboratory, Technical Report, May 2019. [Online]. Available: <https://www.nrel.gov/docs/fy19osti/72856.pdf>

- [23] B. L. Kistler, "A User's Manual for DELSOL3: A Computer Code for Calculating the Optical Performance and Optimal System Design for Solar Thermal Central Receiver Plants," Sandia National Lab, Technical Report, Nov. 1986.
- [24] "The Chemical Engineering Plant Cost Index ®." 2022. [Online]. Available: <https://www.chemengonline.com/pci-home>
- [25] "Ankerlig and gourikwa power stations technical brochure.," ESKOM, Technical Report. [Online]. Available: <https://www.eskom.co.za/wp-content/uploads/2022/04/GS-0003-AnkerligGourikwa-Technical-Brochure-Rev-9.pdf>
- [26] S. Clark, C. McGregor, and J. Van Niekerk, "Using liquefied petroleum gas to reduce the operating cost of the ankerlig peaking power plant in south africa.," J. Energy South. Afr., vol. 33, no. 2, pp. 15–23, May 2022, doi: <https://dx.doi.org/10.17159/2413-3051/2022/v33i2a13453>.
- [27] U.S. EIA, "Carbon Dioxide Emissions Coefficients." Sep. 07, 2023. [Online]. Available: [https://www.eia.gov/environment/emissions/co2\\_vol\\_mass.php](https://www.eia.gov/environment/emissions/co2_vol_mass.php)
- [28] South African DMRE, "Breakdown of petrol, diesel and paraffin prices as at 04 September 2024." Sep. 04, 2024. [Online]. Available: <https://www.dmre.gov.za/Portals/0/Resources/Fuel%20Prices%20Adjustments/Fuel%20Prices%20Per%20Zone/2024/Sep-tember%202024/Breakdown-ofPrices.pdf?ver=M0NnulGPdV06UEycdvJouq%3d%3d>
- [29] South African DMRE, "Diesel Price Margins." Sep. 04, 2024. [Online]. Available: <https://www.dmre.gov.za/Portals/0/Resources/Fuel%20Prices%20Adjustments/Fuel%20Prices%20Per%20Zone/2024/September%202024/Dieselmar-gins.pdf?ver=swiFfvb36tMwhPH08B9w7g%3d%3d>